NANO LETTERS

2007
Vol. 7, No. 3
552−556

Nanofluidic Diode

Ivan Vlassiouk and Zuzanna S. Siwy*

Department of Physics and Astronomy, University of California, Irvine, Irvine, California 92697

Received December 12, 2006; Revised Manuscript Received January 11, 2007

ABSTRACT

We present a nanofluidic diode that at voltage range −5 to +5 V rectifies ion current with degrees of rectification reaching several hundreds. The diode is based on a single asymmetric nanopore whose surface was patterned so that a sharp boundary between positively and negatively charged regions is created. This boundary defines a zone that is enriched with positive and negative ions or creates a depletion zone. The principle of operation of the nanofluidic diode is analogous to that of a bipolar semiconductor diode.

Introduction. Recent development of nanofabrication techniques opened up new possibilities to prepare synthetic nanopores with various shapes, diameters down to 1 nm, and tailored surface charge.[1−4] The interest in nanopores has been triggered by possible application of these systems to single molecules, e.g., DNA detection,[5] chemical sensing and biosensing,[6,7] drug delivery,[8] and nanofluidics.[2,4,9−12] For building devices with controlled mass transport, nanopores seem to be the perfect choice. It is the dramatic increase in surface to volume ratio of these objects that gives access to the phenomena that are not detectable on the microscale. There are three major mechanisms for gaining control of mass transport in nanopores: (i) *volume exclusion principle*, based on proportionality of the total flux to the effective cross section area of the nanopore,[6,7,13] (ii) *hydrophobic interactions* discussed for biological[14] and synthetic nanopores,[15] and (iii) *electrostatic interactions*. In this Letter we will focus on the third effect, i.e., electrostatic interactions of permanent surface charges of nanopores with ions in the background electrolyte solution. We show application of these interactions in designing of a nanofluidic diode based on an asymmetric nanopore prepared in a polymer membrane. We demonstrate operation of this diode in KCl solutions at concentrations between 10 mM and 1 M KCl.

There are only a few examples of nanopores that exhibit diode-like current−voltage ($I-V$) curves at symmetric electrolyte conditions. We and others showed that asymmetric, conically shaped nanopores with permanent surface charges (Figure 1A) rectify ion current.[16−21] Rectification ratio f_{rec} for these nanopores, defined as a ratio of currents recorded for voltages of the same amplitude but opposite polarities, does not exceed at the voltage range −3 to +3 V a factor of $f_{rec} \cong 10$. This effect of rectification is caused by an intrinsic asymmetry of the electrochemical potential of these nanopores.[18,22,23]

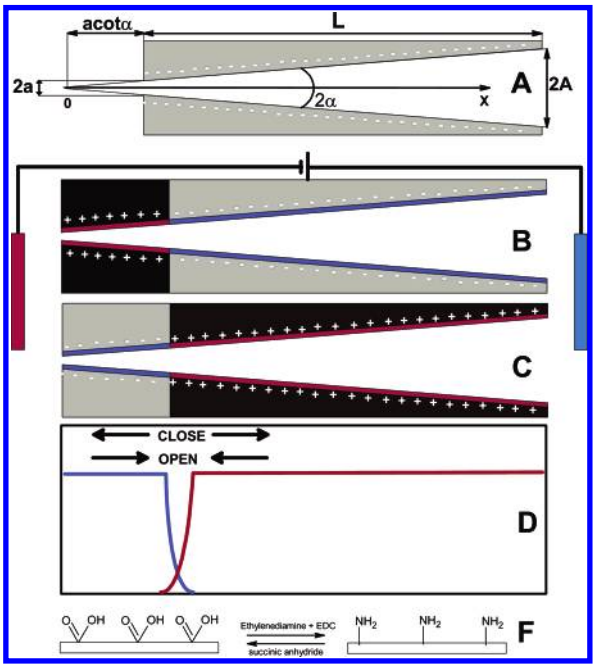

Figure 1. (A) Schematic of a conical nanopore in PET foil: L is the nanopore length, a is tip radius, A is base radius, α is opening angle of a cone. $x_{tip} = a \cot \alpha$, $x_{base} = L + a \cot \alpha$. Surface of nanopores obtained by the track-etching technique possesses carboxyl groups at the density of ≅1 e/nm^2. (B, C) Patterns of surface charge that lead to formation of a nanofluidic diode. (D) Schematic concentration profiles with no applied voltage of positive (red) and negative (blue) ions for a diode shown in (B). (F) Modification chemistry applied to transform carboxyl groups into amino groups by EDC coupling agent. Resulting surface amines are transformed back to carboxyls by succinic anhydride.

In order to create a system that rectifies ion current with much higher degrees of rectification, we had to introduce a possibility to control the concentration of available charge carriers inside nanopores. The ionic diode that we present here is analogous in its operation to a semiconductor bipolar

10.1021/nl062924b CCC: $37.00
Published on Web 02/21/2007

diode, and its design has been stimulated by theoretical predictions shown in ref 12. Our system is also a realization of bipolar membranes systems with well-defined single nanopore geometry.[24−26]

Nanometer size of pores plays a crucial role in design of the diode. If the pore diameter is comparable to the Debye length, ionic distributions inside nanopores are determined by the relation between surface charge density of the nanopores σ (C/m^2), pore radius, and bulk ionic concentrations c_{bulk}. Debye length $1/\kappa$ determines the distance from the pore walls over which the mobile counterions in the electrolyte solution screen the electric fields created by the surface charge. For a nanopore with $\kappa a \cong 1$, where a is a pore radius for cylindrical geometries or a half-height for rectangular pores, the number of counterions to the surface charge will be higher than the number of co-ions inside the pore. Additionally, if the condition $|\sigma| > ec_{bulk}a$ is fulfilled, the number of counterions in a pore will exceed their bulk concentration, resulting in dominant influence of the counterions in the measured current. This effect has been employed in preparation of nanofluidic transistors.[9−11] If the surface of the pore is patterned so that there is a zone with permanent positive surface charges and a part of the pore with negative surface charges (Figure 1B,C), the boundary between these two sections will create a transition zone similar to a pn junction in a semiconductor diode (Figure 1D).

Results. (A) Template Nanopores for Nanofluidic Diode. For a diode template we used well-characterized single conical nanopores (Figure 1A) in 12 μm thick poly(ethylene terephthalate) (PET) membranes prepared by the track-etching technique.[17,18,27] The opening diameters of the nanopores used in these studies were $a \cong 2.5$ nm as measured by an electrochemical method, and $A = 500$ nm, respectively. The small opening of the pore is called the tip, the big opening of the pore is called the base. The template PET nanopores have excess surface charge due to the presence of carboxyl groups created during the fabrication process with estimated surface charge density of $\sim$1 e/nm^2.[17,18] This surface charge density assures that at the tip of a pore with $a \cong 2.5$ nm the concentration of mobile counterions—in our case potassium ions—has to be $|\sigma|/ea \cong 0.67$ M to ensure electroneutrality of the system. It is therefore very easy in our system to achieve a situation when the concentration of counterions in the nanopore is higher than that in the bulk.

(B) Targeted Surface Modification. In order to achieve surface charge distributions shown in Figure 1, we developed a procedure to pattern the surface. Our method of modification relies on a constant in time concentration gradient that is created in a nanopore when a reagent is placed only on one side of the membrane. Targeted modification of the tip requires that concentration of the reagent c in this region is high and decays rapidly along the pore axis x. It is when the conical geometry of the pore becomes critical for building of the nanofluidic diode: conical geometry produces such concentration distribution in a natural way. The steady-state solution of the diffusion equation when $a \ll A$[28] with boundary conditions $c(a\ cot\ \alpha,t) = c_0$, $c(L,t) = 0$ has the following form

$$c(x) = c_0 \frac{a}{A}\left(\frac{L}{x} - 1\right) \qquad (1)$$

$$a \cot \alpha \le x \le L$$

where α is the angle of nanopore's opening (Figure 1A) and $c(x)$ is concentration of the reagent at a position x.

A second important process for the chemical modification of pore walls is binding of the chemical to the surface. We assume that this binding follows the Langmuir isotherm, $\theta = 1 - e^{-C(x)kt}$, where θ is fraction of the surface coverage by the modifying chemical, k is the reaction rate of the chemical with the surface, and t is time. Equation 2 defines the nanopore coordinate (x) along the pore axis with a given surface coverage (θ)

$$x = \frac{c_0 aktL}{c_0 akt - A \ln(1-\theta)} \qquad (2)$$

Point x_0 ($\theta = 0.5$) is the only point with a total zero charge, given by

$$x_0 = \frac{c_0 aLkt}{c_0 akt + A \ln(2)} \qquad (3)$$

Consequently, the surface charge density ($\sigma(x)$) has opposite signs at $0 \le \theta < 0.5$ ($x > x_0$) and $0.5 < \theta \le 1$ ($x < x_0$). The modification of surface carboxyl groups, which possess a negative charge at pH >4, is done by a standard organic chemistry procedure with coupling agent 1-ethyl-3-[3-(dimethylamino)propyl]carbodiimide hydrochloride (EDC).[28] Surface amination can be done from water solutions, providing the possibility of "in situ" monitoring of $I-V$ curves. Once aminated, the nanopore surface can be returned to a negative charge state by reaction with succinic anhydride, forming the carboxyl groups once again (Figure 1F). Such conversion could be done in series numerous times.

(C) Current−Voltage Curves of Nanopores with Homogeneous Surface Charge. A characteristic $I-V$ curve for an unmodified pore, therefore a pore with negative surface charge, is shown in Figure 2A, trace b. Here and later in the text, the grounded electrode was on the tip side. The potential differences were computed as $V_b - V_t$ where V_b and V_t are potentials of the electrodes on the base and tip sides, respectively. By conversion of all carboxyls to amines, the rectification changes its direction due to change of $\sigma(x)$ sign (Figure 2A, trace a).[20] The factor f_{rec} at 5 V for fully aminated and carboxylated pore is constant at pH range <4 to >7 and equal to $\cong$5.[28] Due to the pK_a and pK_b of surface groups, the rectification becomes weaker at solutions of pH <4 in case of pore walls with carboxyls and at pH >7 for aminated surfaces. Thus, at 4 < pH < 7, $\sigma(x)$ for both aminated and carboxylated surfaces reaches its maximum.

(D) Current−Voltage Curves of Nanofluidic Diodes. In order to achieve surface charge distribution shown in Figure

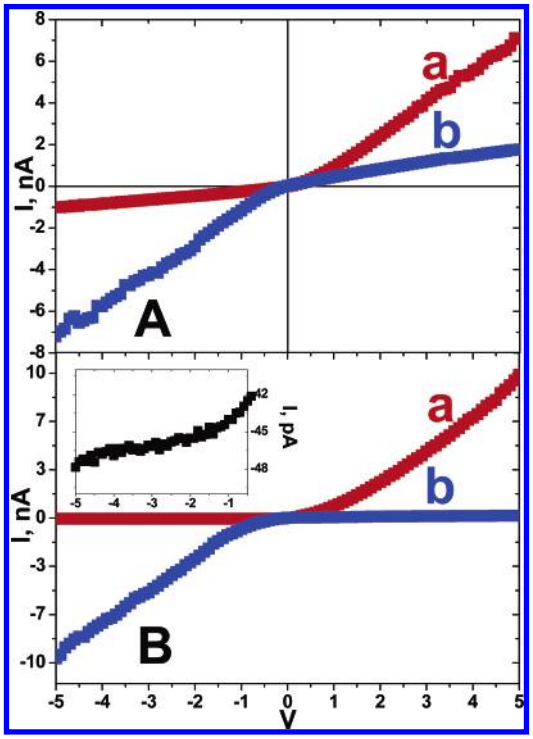

Figure 2. (A) Current−voltage curves for a nanopore modified with amines (a), rendering the surface positively charged, and with carboxyls (b), rendering the surface negatively charged. (B) Current−voltage curves for a nanofluidic diode: curve a corresponds to positive tip and negative base, as shown in Figure 1B (left inset shows zoomed negative currents); curve b corresponds to inverse modification shown schematically in Figure 1C.

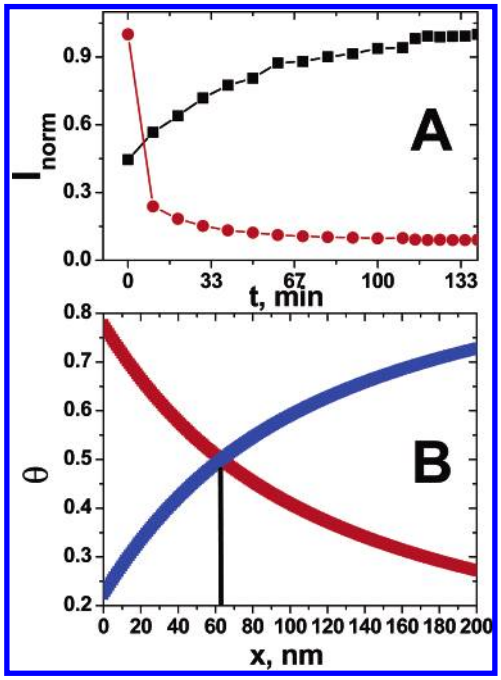

Figure 3. (A) Kinetics of diode formation for surface charge distribution shown in Figure 1B. Solutions of EDC and diamine were introduced on a tip side of the membrane. Negative (red circles) and positive (black squares) currents vs time, normalized with respect to values of current at 2 V. (B) Surface densities of amino (red line) and carboxyl (blue line) groups calculated from eq 2, after 10 min of modification. Black line shows the point of zero charge (x_0)

1B, we applied an ethylenediamine solution with EDC only on the tip side of the membrane, recording $I-V$ curves during the modification. After 2 h, the degree of rectification saturated (Figure 3). An $I-V$ curve recorded for this system is shown in Figure 2B and demonstrates an exceptional rectification ratio ($|I_{5V}/I_{-5V}|$) of 217 times at 0.1 M KCl, pH 5.5. For positive voltages, the current increases with voltage according to a power law: $I \propto V^{1.5}$. The inset in Figure 2B shows that the current for negative voltages remains on the tens of picoamperes level and is practically independent of the voltage.

As the next step, we applied the solution of amines with EDC on the base side of the membrane, which resulted in modification of the whole surface. The degree of rectification of this system was back to the value ≅7. This pore was subsequently subjected to a solution of succinic anhydride placed on the tip side. This modification led to an inverse $I-V$ curve that is shown in Figure 2B, with $f_{rec} \cong 61$. This rectification degree is significantly higher compared to curves shown in Figure 2A, but it is smaller compared to the situation corresponding to the positive tip of the pore. We think that this decrease of f_{rec} could indicate an incomplete amine to carboxyl transformation.[28]

Ion concentration profiles are shown schematically in Figure 1D in order to illustrate the physical basis behind functioning of the nanofluidic diode. The requirement of electroneutrality of the whole system determines the difference in K^+ and Cl^- concentrations ΔC as $\Delta C(x) = 2\sigma(x)/Fr$, where F is the Faraday constant and r is the pore radius at a given position x. At the pore tip with excess positive surface charges, concentration of Cl^- has to be higher than K^+ concentration. In the remaining part of the pore the situation is reversed: due to the negative surface charge, K^+ concentration is higher. Applying voltage of opposite polarities results in dramatically different net concentration profiles. Positive voltages drive K^+ to the tip side and Cl^- to the base, resulting in overlapping of the concentration profiles, large ionic currents, and an open state of the nanopore. Negative voltages move K^+ and Cl^- in the outward direction from the pore, causing formation of a depletion zone and, consequently, a very low conductance of the nanopore.

Discussion. In order to understand the processes behind the strong ionic rectification, we investigated more carefully kinetics of the diode formation. Current−voltage curves were recorded every 5 min when modifying a nanopore from one side using a solution of amines in 0.1 M KCl.[28] Figure 3A shows currents recorded at positive and negative voltages, normalized with respect to either final (positive voltages) or initial (negative voltages) currents at 2 V. A dramatic decrease in values of negative currents, indicating formation of a depletion zone, happens during the first minutes of the reaction. The positive currents show a more gradual increase in time that corresponds to additional attachments of amino groups, resulting in enhancement of Cl^- concentration at the pore tip.

We also studied kinetics of the surface modification reaction when the reaction solution of EDC and amines was

placed on both sides of the membrane. We again recorded $I-V$ curves of a nanopore every 5 min looking for the time required to achieve $\theta = 0.5$, i.e., when the system ceased rectifying. For our nanopore, we had to wait ≅10 min to observe a linear $I-V$ curve. Using first-order reaction kinetics: $e^{-Ckt} = 0.5$ and $t = 10$ min, gave a rate constant of $k = 0.05\ M^{-1}\ s^{-1}$. Because diffusion time of the reagent through the whole pore is $t_{diff} = L^2/D$, assuming $D \cong 10^{-6}$ cm^2/s, one gets $t_{diff} = 1.5$ s. Comparison of the time scales of the modification reaction (10 min) and t_{diff} suggests that the chosen modification chemistry is indeed limited by the reaction rate rather than a diffusion time.

The value of k was the first step for finding the point of zero surface charge x_0. For a cylindrical nanopore, at low voltages, the point x_0 determines the position of the depletion zone center. We would like to point that width of the depletion can change with applied voltage, as shown for bipolar membranes[24] and rectangular nanopores.[12] For a symmetrical nanopore, the depletion zone center should always be located at x_0. Using the experimental parameters $c_0 = 0.05$ M, $k = 0.05\ M^{-1}\ s^{-1}$, $a = 2.5$ nm, $A = 500$ nm,[28] $t = 10$ min, and $\alpha = 2.4$, eq 3 yields $x_0 = 63$ nm, measured from the nanopore tip. We treat this value as an estimation for the position of the center of the depletion zone in our conical nanopores as well. The surface densities of amines and carboxyls corresponding to these parameters are shown in Figure 3B. This distribution of surface charge indicates that a complete coverage of the surface by amines is not required for formation of a good depletion zone. Equation 3 also suggests that velocity of moving of the position x_0 during modification is constant if $c_0akt \ll A \ln(2)$. For experimental parameters used here this inequality is satisfied during the first ~20 min, and the corresponding velocity is equal to 0.2 nm/s. Since the velocity is directly proportional to c_0, we have a possibility to tune x_0 with a high precision. Our nanopore is not symmetrical, thus x_0 as determined from eq 3 is only an estimate of position of the depletion zone center. Experimental data with bipolar membranes as well as theoretical considerations for these systems indicated a possibility of a big shift of the depletion zone in the pore for higher applied bias voltages.

Functionality of our nanofluidic diode is dependent on surface charge of the nanopore that is regulated by pH of the background electrolyte solution. We checked rectification of the diodes shown in Figure 1B,C at pH range <2 to >9 (Figure 4A). Maximum values of f_{rec} were recorded at pH range <4 to >7, therefore the range with maximum surface charge densities.

The formation of a depletion zone could be explained by two effects: (i) electroosmosis or/and (ii) electrophoresis. At negative voltages, electroosmosis forces water to flow out from the pore in both positive and negative nanopore parts. This causes formation of a negative pressure at x_0,[12] and most probably an ion concentration drop as well. When the Debye length is wide enough to exclude co-ions from the nanopore, electrophoresis could also pull the ions with opposite charges in the outward direction from the nanopore forming a depletion zone. In order to check which of these

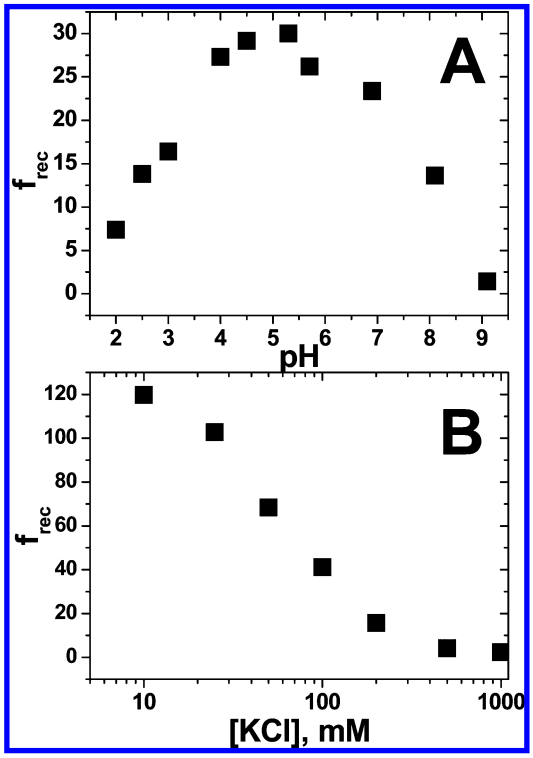

Figure 4. Dependence of rectification degree f_{rec} at +2/−2 V for a nanofluidic diode shown in Figure 1B on pH and concentration of KCl solutions. (A) Recordings were performed in 0.1 M KCl. (B) Recordings were performed at pH = 5.5 and KCl concentrations between 10 and 1000 mM.

two phenomena plays a dominant role in formation of the depletion zone, we performed $I-V$ curve measurements at a broad range of KCl concentrations. We found that the rectification factor f_{rec} decreases by 2 orders of magnitude in the range of KCl concentrations between 10 mM and 1 M. As this range of concentrations, Debye length $1/\kappa$ is changing from 3 to 0.3 nm; i.e., $1/\kappa$ is varying from a value comparable to the radius of the pore tip, to a significantly smaller value. This finding suggests that it is the electrophoresis that plays a dominant role in formation of the depletion zone. It is because electroosmosis exists at high ionic strengths like 1 M KCl.[29]

We would like to point that our system reminds functioning of bipolar membranes whose rectifying properties have been a subject of intensive experimental and theoretical studies.[24−26] A characteristic feature of bipolar membranes is presence of so-called "punch-through" effect observed as a current increase at high reverse bias voltages. This increase of current is associated with contribution of protons and hydroxyl ions generated by high electric field in the depletion zone.[26] At the voltage range that we used in our measurements, this effect was however not observed.

Conclusions. We presented a system of a nanofluidic diode which exhibits rectification according to a mechanism analogous to that of a bipolar diode. We achieved degrees of ion current rectification equal to several hundreds at voltages between −5 and +5 V. This device can be of enormous interest in nanofluidics as well as a starting point for building ionic equivalents of electron devices, such as triodes and transistors.

Acknowledgment. Irradiation with swift heavy ions was performed at the Gesellschaft fuer Schwerionenforschung (GSI), Darmstadt, Germany. Discussions with Professor Ken Shea and Dr. Christina Trautmann are greatly acknowledged. We are grateful to the Institute of Complex Adaptive Matter for financial support.

Supporting Information Available: Experimental procedures including preparation of nanopores and chemical modification of pore surfaces and discussions of dependence of rectification properties of unmodified PET pores on KCl concentration, steady-state solution, rectification ratio vs pH for fully carboxylated and aminated nanopores, estimation of the width of the depletion zone, and reaction rate. This material is available free of charge via the Internet at http://pubs.acs.org.

References

(1) Li, J.; Gershow, M.; Stein, D.; Brandin, E.; Golovchenko, J. A. *Nat. Mater.* **2003**, *2*, 611−615.
(2) Plecis, A.; Schoch, R. B.; Renaud, P. *Nano Lett.* **2005**, *5*, 1147−1155.
(3) Stein, D.; Kruithof, M.; Dekker, C. *Phys. Rev. Lett.* **2004**, *93*, 035901 (1−4).
(4) Karnik, R.; Castelino, K.; Majumdar, A. *Appl Phys. Lett.* **2006**, *88*, 123114 (1−3).
(5) Li, J.; Stein, D.; McMullan, C.; Branton, D.; Aziz, M. J.; Golovchenko, J. A. *Nature* **2001**, *412*, 166−169.
(6) Siwy, Z.; Trofin, L.; Kohli, P.; Baker, L.; Trautmann, C.; Martin, C. R. *J. Am. Chem. Soc.* **2005**, *127*, 5000−5001.
(7) Vlassiouk, I.; Takmakov, P.; Smirnov, S. *Langmuir* **2005**, *21*, 4776−4778.
(8) Desai, T. A.; Hansford, D. J.; Kulinsky, L.; Nashat, A. H.; Rasi, G.; Tu, J.; Wang, Y.; Zhang, M.; Ferrari, M. *Biomed. Microdev.* **1999**, *2*, 11−40.
(9) Daiguji, H.; Yang, P.; Majumdar, A. *Nano Lett.* **2004**, *4*, 137−142.
(10) Karnik, R.; Fan, R.; Yue, M.; Li, D.; Yong, P.; Majumdar, A. *Nano Lett.* **2005**, *5*, 943−948.
(11) Fan, R.; Yue, M.; Karnik, R.; Majumdar, A.; Yang, P. *Phys. Rev. Lett.* **2005**, *95*, 086607 (1−4).
(12) Daiguji, H.; Oka, Y.; Shirono, K. *Nano Lett.* **2005**, *5*, 2274−2280.
(13) Liu, N.; Dunphy, D. R.; Atanassov, P.; Bunge, S. D.; Chen, Z.; Lopez, G. P.; Boyle, T. J.; Brinker, C. J. *Nano Lett.* **2004**, *4*, 551−554.
(14) Kocer, A.; Walko, M.; Meijberg, W.; Feringa, B. L. *Science* **2005**, *309*, 755−758.
(15) Vlassiouk, I.; Park, C.-D.; Vail, S. A.; Gust, D.; Smirnov, S. *Nano Lett.* **2006**, *6*, 1013−1017.
(16) Wei, C.; Bard, A. J.; Feldberg, S. W. *Anal. Chem.* **1997**, *69*, 4627−4633.
(17) Apel, P.; Korchev, Y. E.; Siwy, Z.; Spohr, R.; Yoshida, M. *Nucl. Instrum. Methods Phys. Res., Sect. B* **2001**, *184*, 337−346.
(18) Siwy, Z.; Fuliński, A. *Phys. Rev. Lett.* **2002**, *89*, 198103 (1−4).
(19) Chen, P.; Mitsui, T.; Farmer, D. B.; Golovchenko, J.; Gordon, R. G.; Branton, D. *Nano Lett.* **2004**, *4*, 1333−1337.
(20) Siwy, Z.; Heins, E.; Harrell, C. C.; Kohli, P.; Martin, C. R. *J. Am. Chem. Soc.* **2004**, *126*, 10850−10851.
(21) Cervera, J.; Schiedt, B.; Ramirez, P. *Europhys. Lett.* **2005**, *71*, 35−41.
(22) Hanggi, P.; Bartussek, R. In *Nonlinear Physics of Complex Systems*; Parisi, J., Mueller, S. C., Zimmermann, W., Eds.; Lecture Notes in Physics 476; Springer: Berlin, 1996; pp 294−308.
(23) Astumian, R. D. *Science (Washington, D.C.)* **1997**, *276*, 917−922.
(24) Coster, H. G. L. *Biophys. J.* **1965**, *5*, 669−686.
(25) Bassignana, I. C.; Reiss, H. *J. Membr. Sci.* **1983**, *15*, 27−41.
(26) Mafe, S.; Ramirez, P. *Acta Polym.* **1997**, *48*, 234−250.
(27) Fleischer, R. L.; Price, P. B.; Walker, R. M. *Nuclear Tracks in Solids. Principles and Applications*; University of California Press: Berkeley, CA, 1975.
(28) Supporting Information.
(29) Lakshminarayanaiah, N. *Equations of Membrane Biophysics*; Academic Press, Inc.: London, 1984; pp 100−105.

NL062924B